Article:
Martinez, R., Todd, I. and Mumtaz, K. (2019) In situ alloying of elemental Al-Cu12 feedstock using selective laser melting. Virtual and Physical Prototyping, 14 (3). pp. 242-252. ISSN: 1745-2759

https://doi.org/10.1080/17452759.2019.1584402

This is an Accepted Manuscript of an article published by Taylor & Francis in Virtual and Physical Prototyping on 15/03/2019, available online: http://www.tandfonline.com/10.1080/17452759.2019.1584402.

In-situ alloying of elemental Al-Cu12 feedstock using selective laser melting

Abstract

This investigation developed selective laser melting (SLM) processing parameters for the in-situ fabrication of an Al-Cu12 alloy from pure elemental blends of aluminium and copper powders. Use of elevated pre-heat temperatures (400°C) created a coarser dendritic cell microstructure consisting of supersaturated Al-rich with a uniform Al_2Cu phase granular microstructure compared to non-pre-heated samples. Al-Cu12 in-situ samples achieved maximum tensile strength values comparable to that of sand cast pre-alloyed Al-Cu12. Processing at elevated pre-heat temperatures created components with higher ultimate tensile strength and ductility compared to standard room temperature-built samples due to it assisting a more complete melting of Al and Cu particles. Additionally pre-heating enabled an artificial age hardening, producing an equilibrium $\alpha + \theta$ microstructure. The creation of an alloy in-situ through use of elemental powder blends represents a low-cost and flexible methodology for exploration of new SLM material compositions and potential candidate materials for semi-solid processing using SLM.

Keywords: Additive Manufacturing, Selective Laser Melting, In-situ alloying

1 Introduction

Selective laser melting (SLM) is a powder-based additive manufacturing (AM) process that uses a laser to melt or fuse layers of metallic powder to produce 3D components. The process begins by spreading metallic powder over a substrate plate at a set layer thickness (20-60µm) using a

roller or wiper (Stwora et al. 2013). A high power laser selectively melts the powder feedstock according to a CAD file data slice, this process is repeated until the component is complete. The most extensively used and researched alloys for SLM included titanium, nickel and iron-based alloys (Popovich et al. 2016). SLM generally allows for increased geometric freedom compared to conventional manufacturing techniques with an increased usage in high value applications within aerospace, automotive and medical sectors (Olakanmi et al. 2015).

1.1 SLM processing of pre-alloyed aluminium

SLM processing of aluminium alloy powders such as AlSi12 and AlSi10Mg (Louvis et al. 2011) have been undertaken with a view to gaining an understanding on their processability and resultant part properties. The effectiveness of SLM processing of materials is a function of physical properties, aluminium is challenging to process due to; poor laser beam absorption, susceptibility to oxidation, high thermal conductivity, high co-efficient of thermal expansion, wide solidification (Olakanmi et al. 2011).

One of the main issues during density optimization of aluminium alloys are Marangoni forces which affect the morphology of the melted tracks at high laser powers and low scanning rates with the agglomerate sizes increasing with increasing laser power or decreasing scan rates (Olakanmi et al. 2015). Investigations have shown that for AlSi10Mg the laser power and interaction between the scan speed and scan spacing have a major influence on porosity development (Read et al. 2015). Similar findings were reported for Al-Cu-Mg alloys by Zhang (2016) with apparent reduced micro cracking by reducing scan speed.

1.2 In-situ alloy generation using SLM

Within SLM the use of pre-alloyed powders rather than elemental mixes are the de-facto standard due to an improved homogeneity of constituents. However, the ability to create custom alloys by simply mixing elemental blends may create opportunities and flexibility for researchers to quickly manufacture powders at a laboratory scale to assist in new alloy/application development. Exploring new alloy design using this methodology may be more cost-effective than investing in early gas atomisation manufacturing runs for the creation of pre-alloyed powders for initial stages of alloy design/testing.

Limited research has been focused on assessing potential for in-situ alloy creation using SLM. Sisteaga et al. (2016) mixed A7075 pre-alloy with 4% Si elemental powder successfully produced dense crack-free parts.Vora et al. (2017) demonstrated the successful creation in-situ Al-339 by mechanically mixing two custom designed alloys AlMg and SiCuNi, however mechanical properties were not reported. Kang et al. (2017) produced a eutectic in-situ alloy from elemental Al(42µm) and Si (6µm) powders demonstrating mechanical properties that were comparable to AlSi12 processed as a pre-alloy. The patented anchorless selective laser melting (ASLM) method (used to process and maintain materials within a semi-solid state) relies on the use of elemental blends within the process rather than fully alloyed feedstocks (Vora et al. 2014). A further understanding of the properties of in-situ alloyed materials from elemental blends would also assist in expanding the range of alloys/materials available for the ASLM process today.

Recently, increased attention has focus on Al-Cu alloys due to their heat treatable high strength, corrosion resistance, and low density. Hu Zangh et al. (2016) successfully produced high density SLM Al2024 with superior mechanical properties compared to A2024 in an annealed state. Work

published by Ahuja et al. (2014) demonstrated the processability of Al-Cu wrought alloys AW2219 and AW2618 with 99% relative density. Findings of Wang et al. (2018) demonstrated an increase in mechanical properties for in-situ Al-CuX alloys using mixtures of Al4.5Cu pre alloy with pure Cu powders. The aim of this work is to investigate the phases and microstructure of a new Al-Cu alloy for ASLM and the effect of in-situ high temperature processing on mechanical properties.

2 Materials and Methodology

The materials used during this investigation were pure Al and Cu powders supplied by LPW technology. Both powders were mixed by weight percent (wt%) using a mixing ratio of Al: Cu =88:12%Vol, see Figure 1 for the binary phase diagram for alloy. These were blended using a tumbling speed mixer DAC 800 at 800 rpm for 10 minutes. The average particle size of Al and Cu powders were 40µm and 12µm respectively as shown in Figure 2. A commercial SLM Renishaw 125 system with a 200W fibre laser and purged inert argon gas atmosphere was used in this study. The original chamber was fitted with a 125×125×100 mm^3 build volume as standard. For this study a custom high temperature heated bed was designed and integrated into the SLM 125 system. The heated bed is capable of heating the substrate up to 800˚C and is fitted with a 67x67x80 mm^3 build volume. Samples were built at room temperature and 400˚C.

Building with 40µm powder layers, a series of cube samples 5x5x5 mm^3 were produced These were then polished cross-sectioned and etched with a 5% HF (100 ml distilled water, 5 ml hydrofluoric acid) and examined within the parametric porosity optimisation trials as shown in Figure 3(a). The SLM processing parameters for the trials are shown in Table 1. An optical

microscope Nikon eclipse LV150, fitted with Buehler Omnimet 9.5 internal software was used to examine images for each sample with an adjusted magnification of 100x. ImageJ software was used to determine the porosity % applying a binary threshold method.

Chemical composition was determined by X-Ray fluorescence spectrometer (XRF) analysis. This procedure was used to determine whether the correct composition was attained within the feedstock before after processing. Scanning electron microscope (SEM) JEOL6610LV was used to perform the microstructure analysis. Phase composition analysis was performed using Siemens-500 X-Ray Diffraction (XRD) with Cu Kα radiation. Micro-hardness was measured with a load of 25 g for 15 seconds with a total of 12 indentations per sample to obtain the average value. Cylinders were built and machined to perform mechanical analysis. Cylinder samples were fabricated using optimized porosity parameters shown in Figure 5, room and high temperature pre-heat was used to process components at 180W and 170W respectively. The tensile tests were carried out at room temperature using a Shimadzu (AG-X) machine according to ASTM E8-16a Method B with a free-running crosshead speed of 2 mm/min.

Table 1. SLM processing parameters

Power(W)	**Exposure(µs)**	**Hatch Spacing(mm)**	**Point distance(µm)**	**Layer thickness(µm)**	**Bed Temperature(°C)**
160,170,180	130-160	0.05, 0.07, 0.09	20-40	40	Room temperature, 400°C

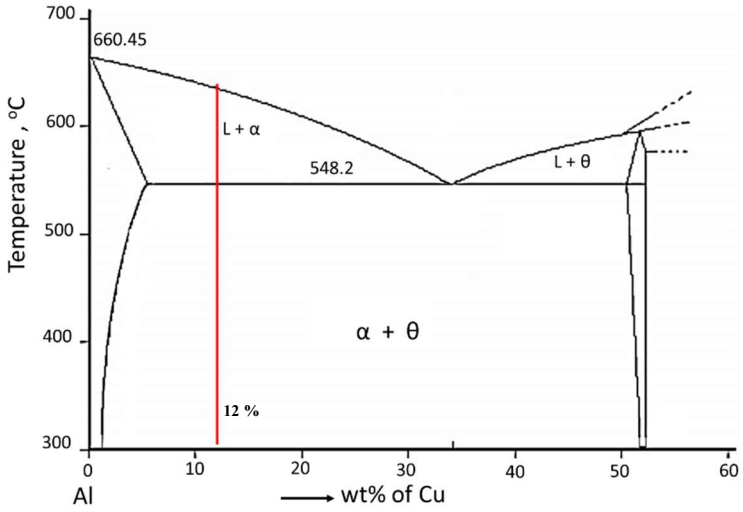

Figure 1. Binary phase diagram Aluminium-Copper

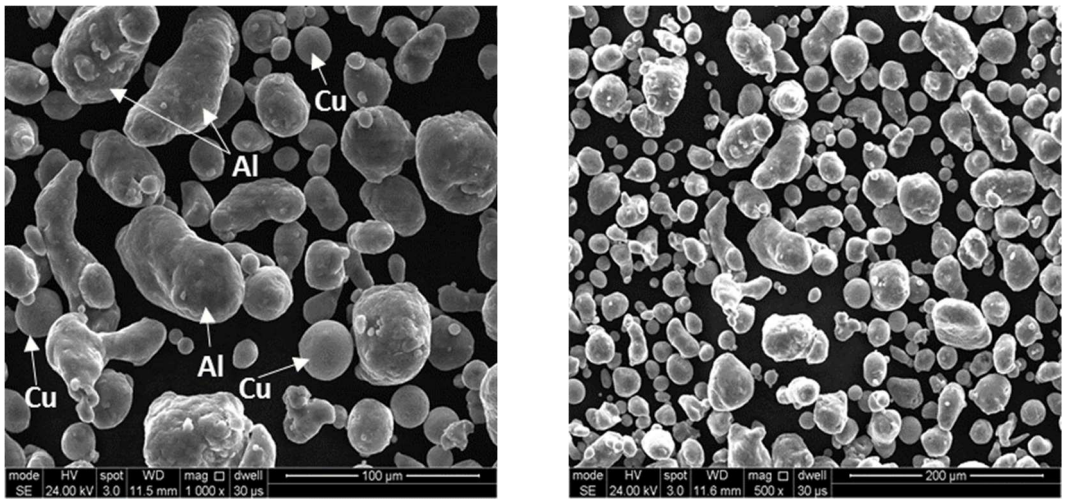

Figure 2. Morphologies of blended aluminium and copper powders at different magnification scale

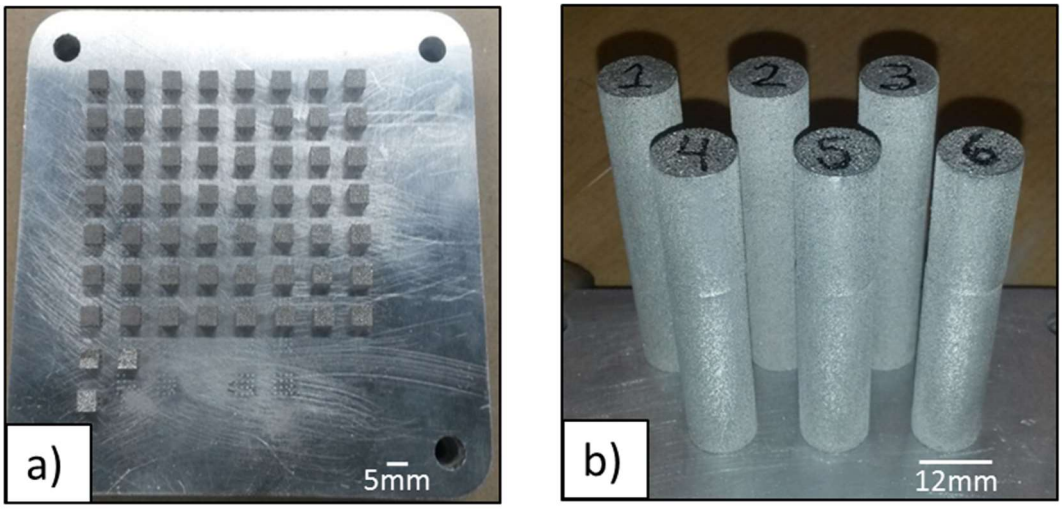

Figure 3. (a) Al-Cu12 in-situ SLM sample cubes 5x5x5 mm^3 and (b) Al-Cu12 in-situ SLM cylinders as built for tensile testing (65 mm height)

3 Results and Discussion

3.1 Porosity

Using design of experiments, a total of 90 samples were created from the Al-Cu12 elemental blends and analysed for porosity, chemical composition and microstructure. Figure 4 shows the relative density of fabricated samples as a function of Scanning Speed (SS) in mm/s for three different values of laser power (160,170,180 Watts). Each specimen was cut and polished cross-sectioned perpendicular to building direction. All trials were divided into 3 batches, fixing the Laser Power(LP), with Point of Distance (POI) and Exposure Time (ET) varied. A relative density of 96-99.5% was achieved in samples that used the lowest laser scan speed with the highest laser power of 180W, a similar trend could be observed in the samples using lower powers. As expected it was found that due to the high reflectively and thick oxides present on the surface of aluminium,

higher energy densities were required to reduce lack of fusion porosity. Similar affirmation was reported by Olakanmi (2015) and Louvis et al. (2011) , densification was improved as the laser power increased while the scan speed and scan spacing decreased. Moreover, the lower part densities of 86-92% were found with those samples produced using higher scanning speeds, this may be a consequence of using insufficient energy density to melt particles. It was found that using a hatch spacing of 0.07mm and scanning speeds between 119-147mm/s achieved the highest relative density values.

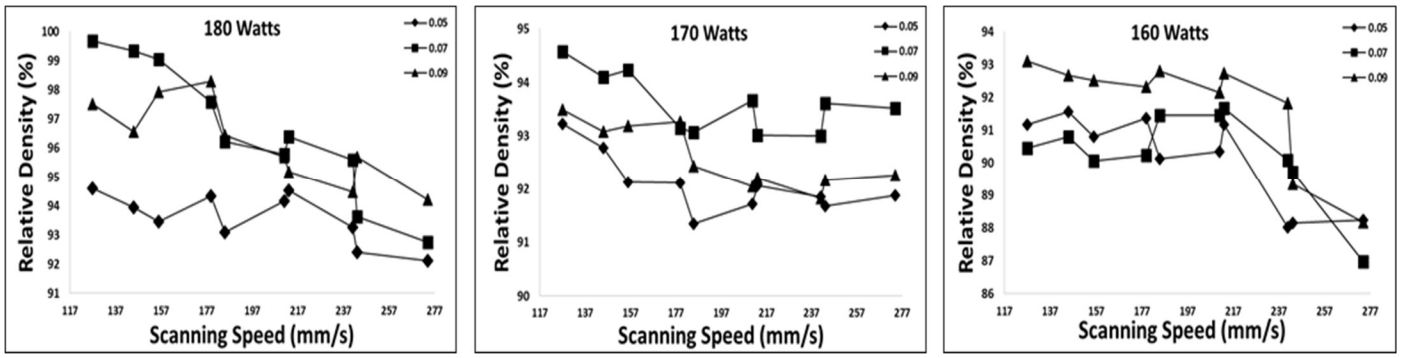

Figure 4. Relative density of SLM processed elemental Al-Cu12 (room temperature), hatch space of 0.05-0.09mm and laser power 160-180W

Table 2 shows a different values of Laser Power (LP) and Exposure time (ET) of the highest and lowest sample porosity attained. For the samples obtained at 160W, it was observed that irregular shaped voids were present, possibly caused by insufficient energy input resulting in a partial melting of powder, this could also be attributed to rapid solidification of aluminium alloy without complete filling the gaps due the velocity of laser processing (Rayleigh instability). There is a difference in void morphology for samples produced using 170W, this may be caused by the oxygen trapped during the melting process. The comparison map shows that, the higher the energy input is in combination with higher exposure time, the higher is the density of the sample.

Table 2. Porosity comparison of SLM processed elemental Al-Cu12, plotted against laser power and exposure time

P(W)/ET(µs)	130	140	150	160
160				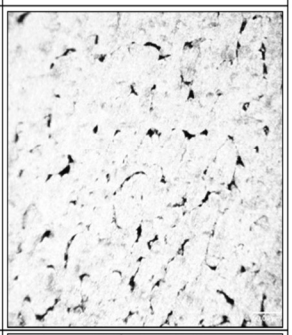
170	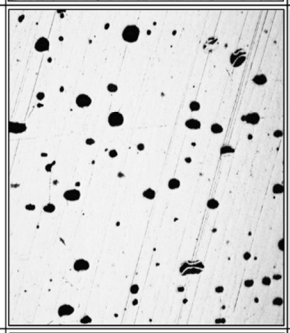	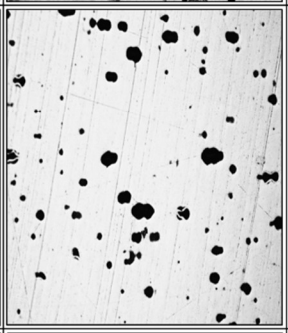	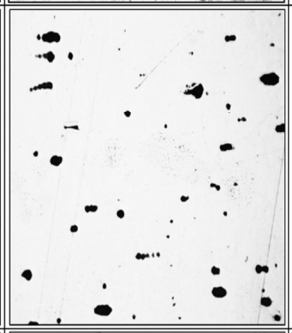	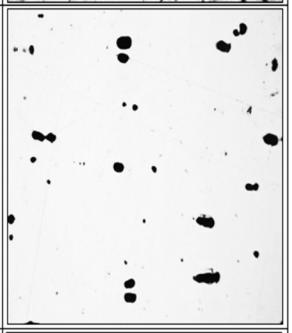
180	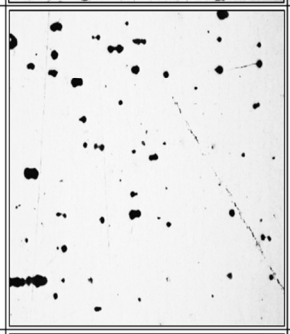		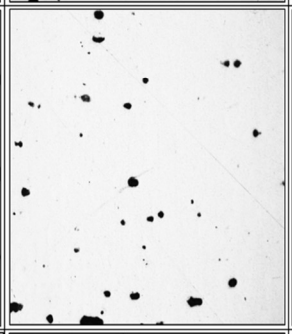	
170 (Heated Bed)	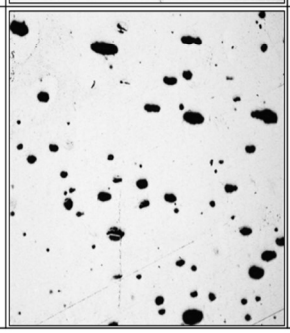		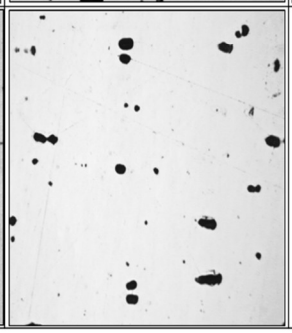	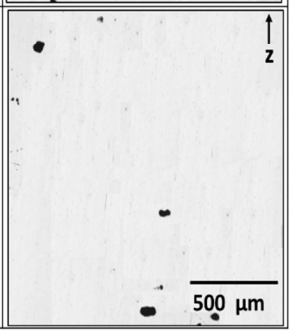

Optimization parameters for elevated pre-heating are different than room temperature samples. At a powder bed pre-heat temperature of 400°C a processing laser power of 170W resulted in a relative density of 99.1% as shown in Figure 5. Using 180W at elevated powder bed pre-heat generated excessive heat input causing evaporation of material, increased porosity and generated an irregular surface (balling) within the processed material.

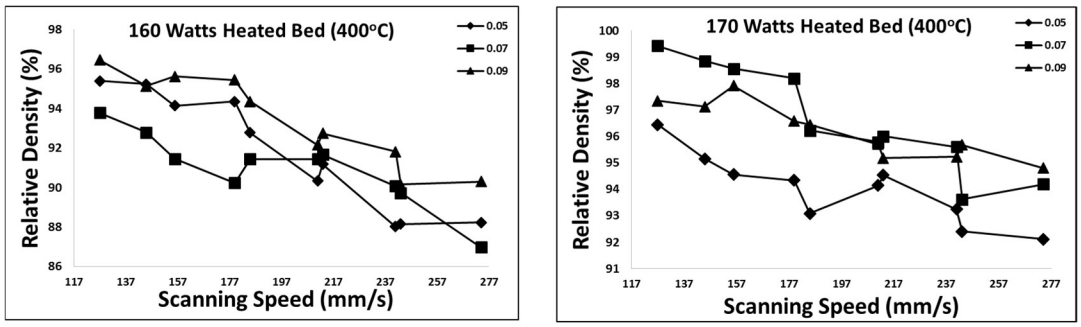

Figure 5. Relative density of SLM processed elemental Al-Cu12 (400°C), hatch space of 0.05-0.09mm and laser power 160-170W

3.2 Phase analysis and microstructure characterization

Phase analysis of Al-Cu12 SLM samples was performed using XRD, the patterns are shown in Figure 6. Al_2Cu intermetallic compound was identified in all samples for room temperature and 400°C, indicating a good alloying between Al and Cu powders. However the peak intensity belonging to Al_2Cu are less, therefore becoming a minor constituent in the Al-Cu12 alloy. XRF analysis was also performed jointly to corroborate initial powder mixing, showing agreement with SLM process chemical composition, XRF results are shown in Table 3 where it is clear to observe that the final part contains an average element mixing ratio within 94% of the expected Al-Cu12

ratio. Elemental loss during SLM processing and/or human error during powder blending can account for this chemical compositional variation between powder and SLM samples, in addition XRF shows a list trace element (e.g Si) resulting from sample preparation.

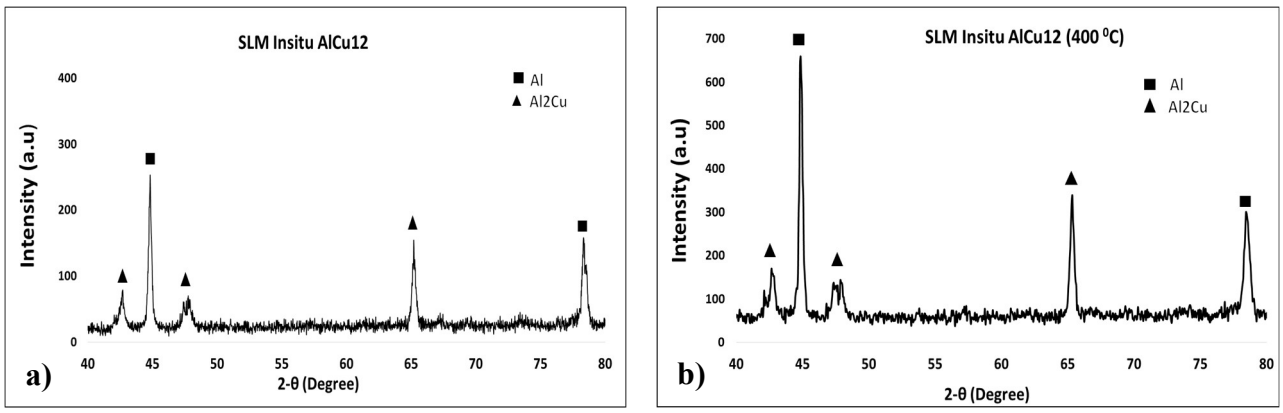

Figure 6. XRD patterns of SLM in-situ Al-Cu12 a) room temperature b) 400 °C

Table 3. X-Ray fluorescence spectrometer analysis of in-situ SLM Al-Cu12 samples

Sample	Al %	Cu %
1 (as built)	82.83	15.21
2 (as built)	85.83	11.71
3 (as built)	85.54	11.98
4 (pre-heat)	84.31	14.08
5 (pre-heat)	84.86	12.77
6 (pre-heat)	85.24	13.06

3.2.1 Low-temperature pre-heated microstructure

Experiments undertaken at room temperature using optimised parameters revealed a hypoeutectic microstructure produced as a result of in-situ alloying of blended Al and Cu powders. Figure 7 shows an optical image of an etched sample showing a dendritic microstructure for Al-Cu12. The primary microstructure observed is a rich α-Al matrix (in light colour) surrounded by a finely Al-Cu eutectic mixture (α and θ), this exhibits the typical directional solidification present in SLM microstructures. Melt pool variable sizes are due to laser scan pattern rotation of 67 degrees. A transition from a finer microstructure to coarse microstructure could be observed from the core of melting pool due to the movement of the heat source. Cu rich zones are observed in some regions, this is likely due to the differences of the melting point for both elements with insufficient laser energy time and Cu limited solute diffusivity in Al. In Figure 8 a non-diffused Cu rich zones are shown (larger than Cu particle size within the feedstock). Also, it is believed that due to the nature of the powder processing (powder blending to layering on powder bed), there would be segregation within the blend that reduces the uniformity of powder feedstock or even agglomeration during the mixing stage (Louvis et al. 2011). This non-uniform build-up of highly reflective Cu powders with high melt temperature (1085°C) in comparison to Al, may create un-melted, un-alloyed defect sites or weakness that will act as a failure points during mechanical testing.

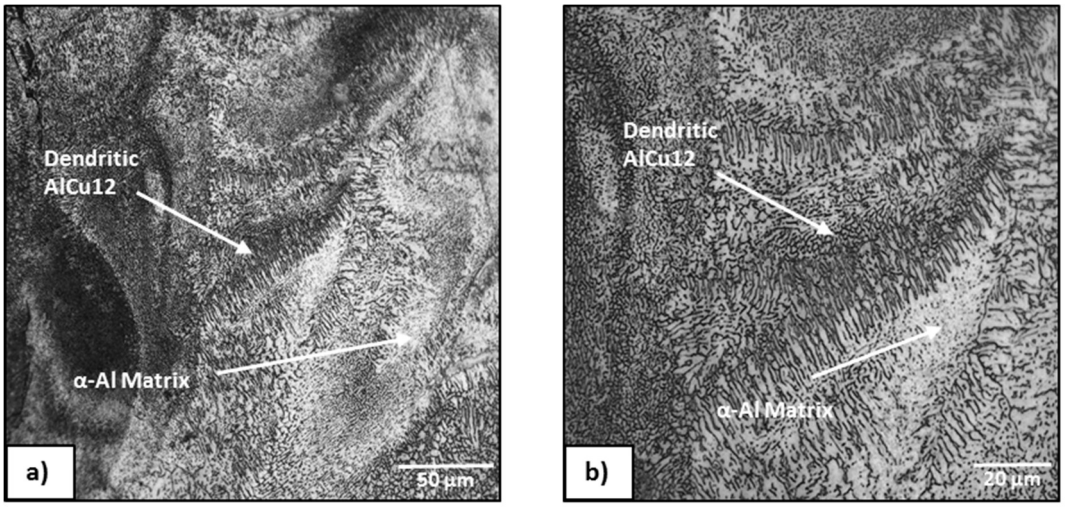

Figure 7. Optical microscope images of etched Al-Cu12 sample showing dendrite orientation a) 20 µm b) 50 µm

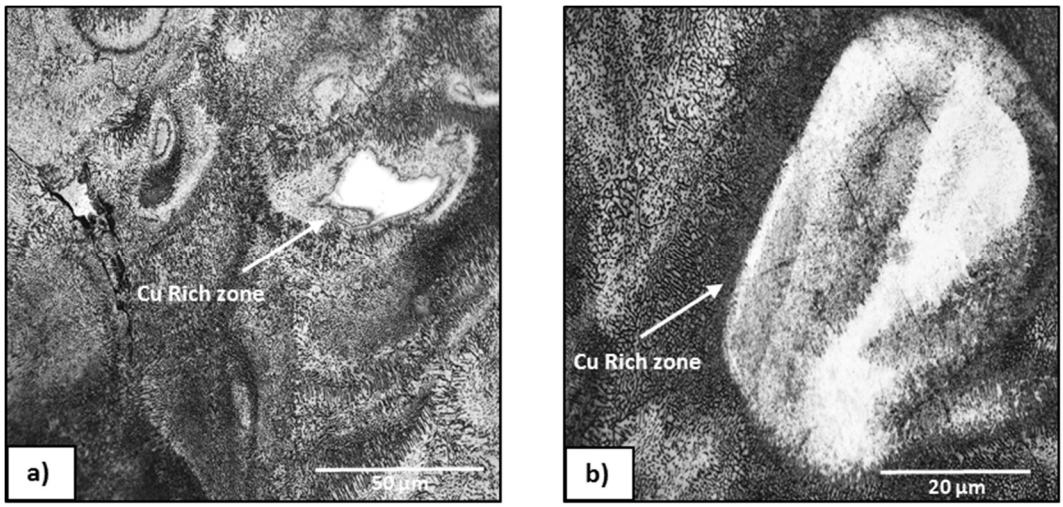

Figure 8. Non-fully diffuse Cu-rich zones at room temperature a) 50 µm b) 20 µm

3.2.2 High-Temperature pre-heated microstructure

Figure 9 shows the polished cross-sections of samples built using high-temperature pre-heating. It can be observed that there is a uniform α-Al matrix with coarser dendritic cells compared to samples built at room temperature powder bed pre-heating. This is a result of the elevated heating and slow cooling to room temperature over a period of 4-5 hours. The α-Al matrix is mainly concentrated in the darker grey areas while the lighter area exhibits a higher α-Al (Cu) content. EDS analysis was performed to observe the distribution of individual elements for the high-temperature samples. Figure 10 shows the results of element mapping where it is possible to differentiate by colour the location of each element. It was found that both elements Al and Cu were uniformly distributed over the analysed cross section, indicating a well-blended uniform microstructure, Al_2Cu phase is distributed in the α-Al matrix with no evidence of Cu rich zones or non-diffused Cu particles. This is may be due to the high pre-heat temperature improving melting

behaviour and allowing the material to remain within its diffusional temperature range while processing.

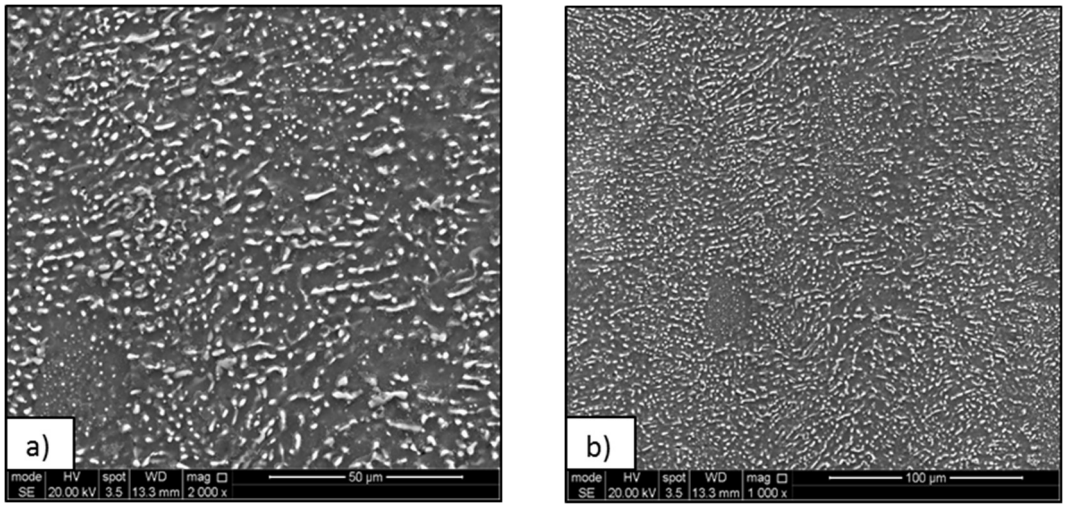

Figure 9. SEM micrographs of in-situ SLM Al-Cu12 samples processed at 400°C, a) 50µm, b) 100µm

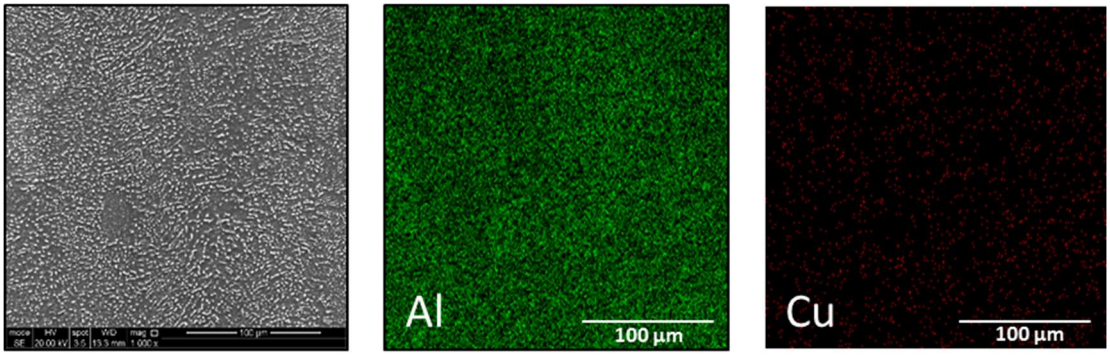

Figure 10. EDS mapping of elements and distribution of Al and Cu for a sample processed at 400° C

When pre-heating the powder bed, the microstructure becomes coarser due to the in-situ annealing processing temperature range. Figure 11 shows a direct comparison between SLM standard and high-temperature built samples.

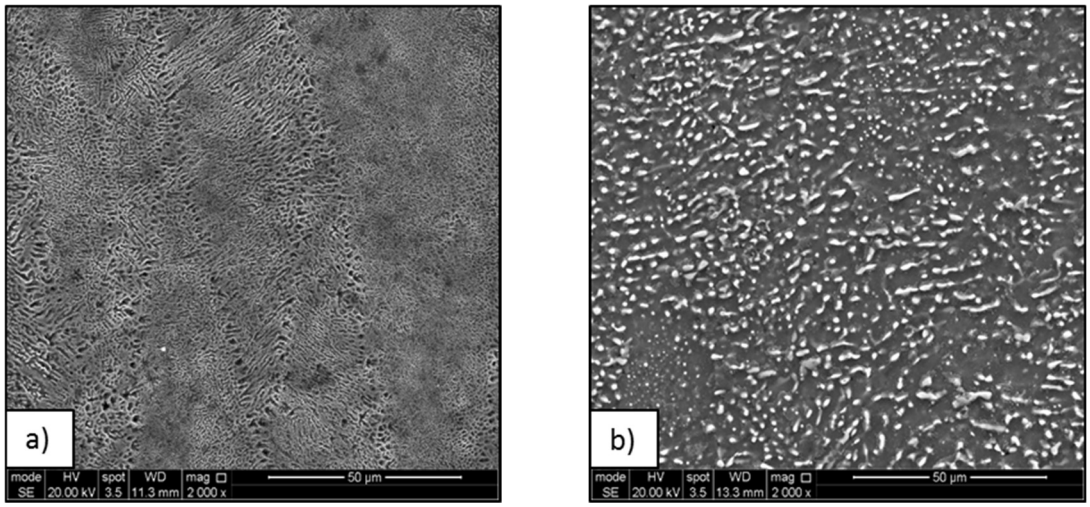

Figure 11. Microstructural comparison of SLM samples, (a) as built with fine eutectic features and (b) high-temperature (400ºC) with uniform coarser microstructure

3.3 Mechanical properties

Reference values for sand and permanent mould aluminium alloys were taken from literature (Mondolfo 1976). Figure 12 shows the micro-hardness (Vickers) of samples, it was observed that there were increases of approximately 11% in hardness with the use of a high temperature pre-heating which are similar to sand casting values (70-90 Hv) and permanent mould (80-120 Hv) AlCu12% alloys. This increase in micro-hardness can be attributed to the more uniform

microstructure and the increasing volume fraction of Al_2Cu intermetallic phase. Figures 13-14 presents the tensile properties of parts (UTS, stress-strain relationship etc.) produced in the z and x axis build orientation at room temperature and high temperature for the SLM in-situ Al-Cu12 alloy. It can be seen that the use of high temperature pre-heating greatly influences mechanical properties. The maximum UTS of 172 MPa (similar to sand casting AlCu12 alloys 120-180MPa) was observed in the high-temperature samples with an x build orientation, this represents an increase of 60% of UTS compared to the standard SLM sample built in the z axis, which exhibits a UTS 103 MPa. It is believed that samples processed at room temperature contained more defects (i.e un-melted Cu particles) than high temperature processed SLM parts and therefore significantly weaker mechanical properties. It is well known that interlayer porosity will increase in z direction specimens due the high number of layers resulting in lower UTS. However even for high temperature samples, the average UTS still falls below that of sand cast AlCu12 alloys and is most likely to be a result of ever present defects within the part (porosity).

Yield strength is inherently poor for the room temperature samples, likely due to presence of defects (un-melted Cu particles) and not fully optimised parameters. Findings reported by Ali et al. (2017) found similar trends for the mechanical properties of pre-heated Ti6Al4V processed by SLM, nevertheless it showed that maximum annealing temperature exhibits a sharp decline of UTS (60%) results regarding the martensitic temperatures. This finding suggests that the results of UTS of the high-temperature samples could be attributed to the coarser grain structure developed during the maximum annealing temperature (310-410°C for Al) which leads to a premature failure under load meanwhile for the room temperature the non-uniform microstructure as well the internal voids and Cu rich zones could create a premature failure. The lower results of elongation could be

attributed to low ductility of Cu rich zones presented in the microstructure and the supersaturated structure presented in Al-based SLM alloys.

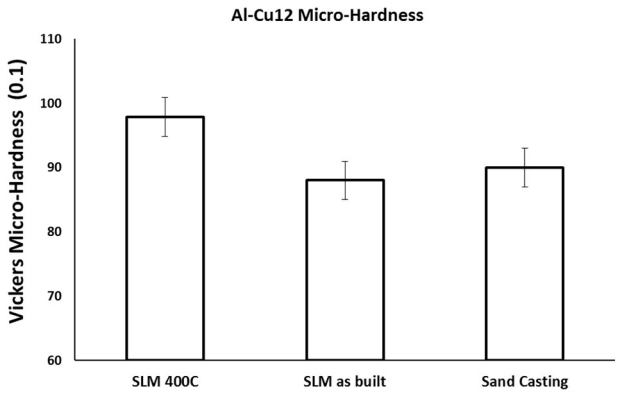

Figure 12. Micro-hardness for In-situ Al-Cu12 at 400°C and room temperature (as-built)

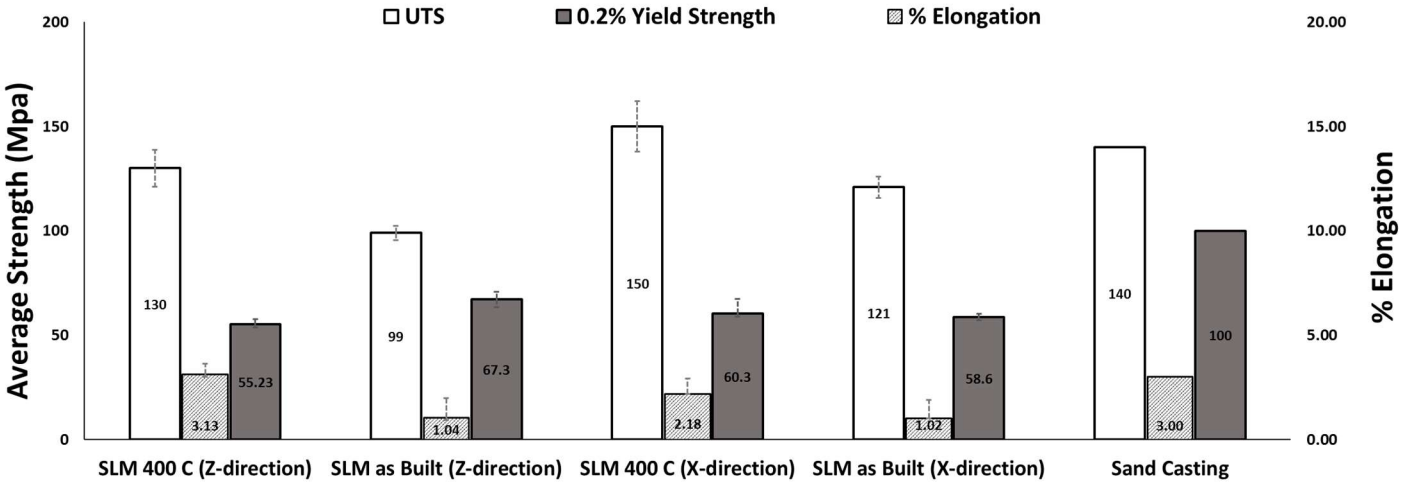

Figure 13. Effect of heated bed temperature on UTS, yield strength and elongation

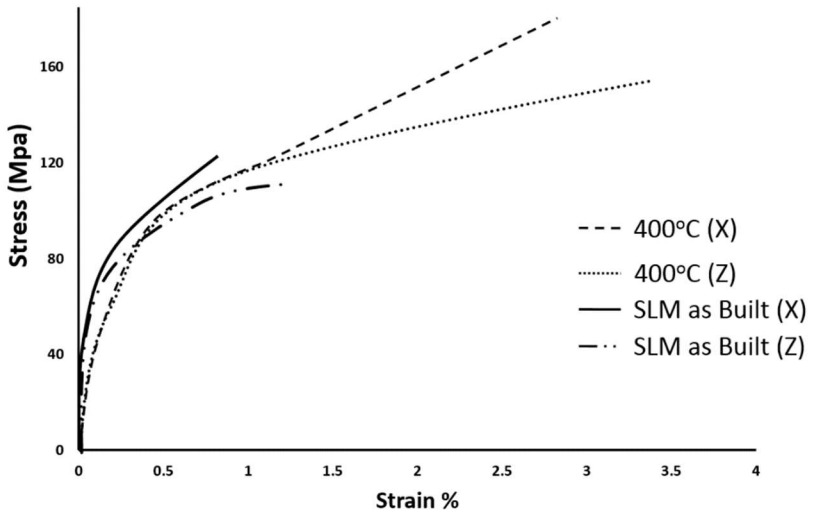

Figure 14. Stress-Strain curve for In-situ Al-Cu12 SLM at different build temperatures and build directions

Figure 15 shows the fracture morphology of the dense (>99.9%) in-situ Al-Cu12 samples built at room temperature and 400°C degrees. The fracture surface observed within the room temperature sample corresponds to a typical ductile fracture (Figure 15a). Figure 15b shows the high magnification image of the fracture zones which reveals the presence of un-melted fine Cu particles distributed along the layer surface, this un-melted distributed of Cu particles within the structure acts as a weakness causing it to fail prematurely leading to poor UTS and elongation. Even though process parameters were optimised to produce >99% density components, there were still difficulties to process the material and fully melt Cu particles, requiring further parameter optimisation. The fracture surface for high-temperature sample shows spherical porosity and internal crack fracture, Figure 15c and Figure 15d shows a higher magnification of the sample where it is possible to observe un-melted particles of Al surrounding the internal crack fracture,

these un-melted Al particles trapped during the laser overlapping process (Marangoni forces) resulting in poor homogeneity in the zone causing the internal crack fracture this once again indicates that despite achieving >99% parts density, processing parameters (or powder size/morphology needs to be optimised to increase packing density) need still be further optimised to manage presence of un-melted powder particles and gas occluded porosity.

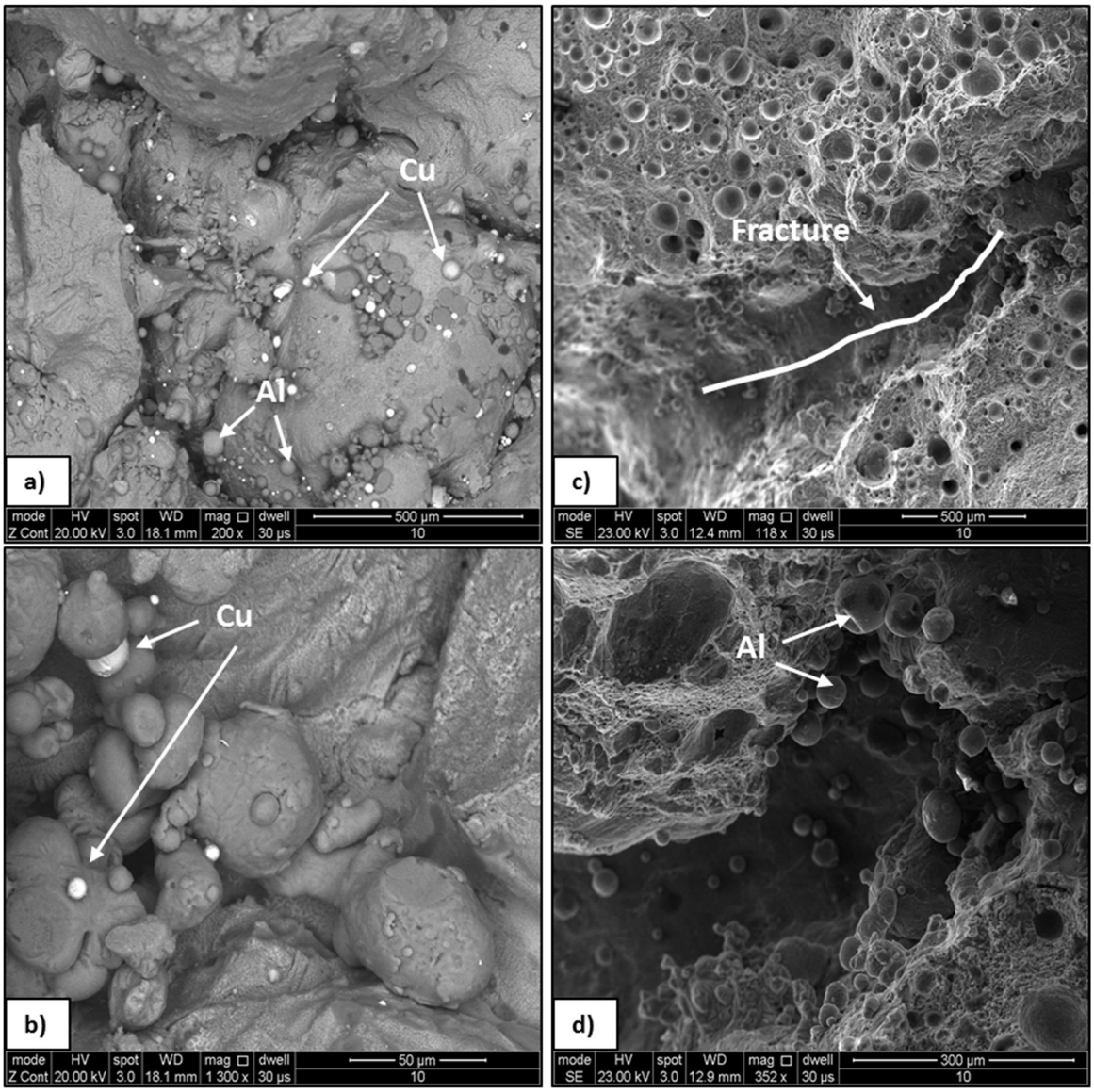

Figure 15. Backscattered SEM micrographs from the tensile fracture surface of In-situ Al-Cu12 SLM a) and b) and high-temperature (400°C) c) and d)

4 Conclusions

SLM parameters were developed to process elemental blends of Al and Cu powder creating a hypo-eutectic Al-Cu12 alloy in-situ. As expected a reduced scanning speed and high energy input were found to improve melting of these highly reflective materials. Cu rich zones were observed in the case of low energy density processing or trials conducted using no powder bed-pre-heating. In-situ Al-Cu12 showed fine supersaturated cellular dendrite microstructure similar to pre-alloys while processing by SLM. Both microstructures consisting in cellular rich α-Al matrix and AlCu-θ as well as the presence of intermetallic Al_2Cu. A finer dendritic cell microstructure was observed for as-built conditions with no pre-heating, meanwhile, a coarser more uniform microstructure was observed for high temperature samples. It was demonstrated that preheating the powder bed to 400^{o}C degrees improved the UTS by 50% with to respect room temperature parts and is comparable with sand and permanent mould casting AlCu12 alloys. Samples built in the X-direction showed better mechanical properties than samples built in the Z-direction. The improvement in UTS are attributed to the homogenized microstructure resulting from the in-situ age hardening during the process and more complete diffusion of elements (i.e Cu). It is theorised that it may be possible to further increase the UTS by reducing the pre-heating temperature to obtain a finer uniform microstructure. The ductility showed a minimum improvement, however the yield strength showed a reduction due to the pre-heat temperatures operating close to the maximum annealing temperature of the material.

The use of elemental powder blends to create alloys in-situ needs to consider particle size/shape (to maximise powder packing density) and blending rigour in order to ensure consistent distributions of elemental powders and break-up of powder agglomerates. Further to this

processing in an un-alloyed state may lead to loss of elements if melting temperature of elements are considerably different. To be comparable with pre-alloyed cast, processing conditions need to be sufficiently optimised to increase component density to >99.9% (achievable with most SLM alloys), remove un-melted Al/Cu powder particles and gas occluded porosity. Clearly the processing of Al and Cu in combination is still a challenge using SLM (highly reflective, thick oxide layers, high thermal conductivity etc.) and requires further development if it's to be considered for engineering applications. However, the blends of Al and Cu powder used within this investigation show early promise for the area of in-situ alloying using SLM and candidate materials for semi-solid processing. This encouragement is derived from the creation of materials in-situ with mechanical properties comparable to that of conventionally manufactured, with microstructures that are generally uniform with chemical compositions similar to that of their pre-alloyed equivalents.

5 References

Stwora, A, and G Skrabalak. 2013. "Influence of Selected Parameters of Selective Laser Sintering Process on Properties of Sintered Materials." Journal of Achievements in Materials and Manufacturing Eingineering 61 (2): 375–80.

Popovich, A., V. Sufiiarov, I. Polozov, E. Borisov, D. Masaylo, and A. Orlov. 2016. "Microstructure and Mechanical Properties of Additive Manufactured Copper Alloy." *Materials Letters* 179: 38–41. https://doi.org/10.1016/j.matlet.2016.05.064.

Louvis, Eleftherios, Peter Fox, and Christopher J. Sutcliffe. 2011. "Selective Laser Melting of Aluminium Components." *Journal of Materials Processing Technology* 211 (2): 275–84. https://doi.org/10.1016/j.jmatprotec.2010.09.019.

Olakanmi, E. O., R. F. Cochrane, and K. W. Dalgarno. 2011. "Densification Mechanism and Microstructural Evolution in Selective Laser Sintering of Al-12Si Powders." *Journal of Materials Processing Technology* 211 (1): 113–21. https://doi.org/10.1016/j.jmatprotec.2010.09.003.

Gu, D D, W Meiners, K Wissenbach, and R Poprawe. 2012. "Laser Additive Manufacturing of Metallic Components: Materials, Processes and Mechanisms." *International Materials Reviews* 57 (3): 133–64. https://doi.org/10.1179/1743280411Y.0000000014.

Olakanmi, E. O., R. F. Cochrane, and K. W. Dalgarno. 2015. "A Review on Selective Laser Sintering/Melting (SLS/SLM) of Aluminium Alloy Powders: Processing, Microstructure, and Properties." *Progress in Materials Science* 74: 401–77. https://doi.org/10.1016/j.pmatsci.2015.03.002.

Read, Noriko, Wei Wang, Khamis Essa, and Moataz M. Attallah. 2015. "Selective Laser Melting of AlSi10Mg Alloy: Process Optimisation and Mechanical Properties Development." *Materials and Design* 65: 417–24. https://doi.org/10.1016/j.matdes.2014.09.044.

Zhang, Hu, Haihong Zhu, Ting Qi, Zhiheng Hu, and Xiaoyan Zeng. 2016. "Selective Laser Melting of High Strength Al-Cu-Mg Alloys: Processing, Microstructure and Mechanical Properties." *Materials Science and Engineering A* 656: 47–54. https://doi.org/10.1016/j.msea.2015.12.101.

Montero Sistiaga, Maria L., Raya Mertens, Bey Vrancken, Xiebin Wang, Brecht Van Hooreweder, Jean Pierre Kruth, and Jan Van Humbeeck. 2016. "Changing the Alloy Composition of Al7075 for Better Processability by Selective Laser Melting." *Journal of Materials Processing Technology* 238: 437–45. https://doi.org/10.1016/j.jmatprotec.2016.08.003.

Vora, Pratik, Rafael Martinez, Neil Hopkinson, Iain Todd, and Kamran Mumtaz. 2017. "Customised Alloy Blends for In-Situ Al339 Alloy Formation Using Anchorless Selective Laser Melting." *Technologies* 5 (2): 24. https://doi.org/10.3390/technologies5020024.

Kang, Nan, Pierre Coddet, Lucas Dembinski, Hanlin Liao, and Christian Coddet. 2017. "Microstructure and Strength Analysis of Eutectic Al-Si Alloy in-Situ Manufactured Using Selective Laser Melting from Elemental Powder Mixture." *Journal of Alloys and Compounds* 691: 316–22. https://doi.org/10.1016/j.jallcom.2016.08.249.

Pratik Vora; Kamran Mumtaz, Ph.D; Iain Todd; Neil Hopkinson. 2014. "AlSi12 In-Situ Alloy Formation and Residual Stress Reduction Using Anchorless Selective Laser Melting." *Elsevier Editorial System* 1 (1): 30.

Ahuja, Bhrigu, Michael Karg, Konstantin Yu Nagulin, and Michael Schmidt. 2014. "Fabrication and Characterization of High Strength Al-Cu Alloys Processed Using Laser Beam Melting in Metal Powder Bed." *Physics Procedia* 56 (C): 135–46. https://doi.org/10.1016/j.phpro.2014.08.156.

Ali, Haider, Le Ma, Hassan Ghadbeigi, and Kamran Mumtaz. 2017. "In-Situ Residual Stress Reduction, Martensitic Decomposition and Mechanical Properties Enhancement through High Temperature Powder Bed Pre-Heating of Selective Laser Melted Ti6Al4V." *Materials Science and Engineering A* 695 (April): 211–20. https://doi.org/10.1016/j.msea.2017.04.033.

Savalani, Monica Mahesh, and Jorge Martinez Pizarro. 2016. "Effect of Preheat and Layer Thickness on Selective Laser Melting (SLM) of Magnesium." *Rapid Prototyping Journal* 22 (1): 115–22. https://doi.org/10.1108/RPJ-07-2013-0076.

Wang, P., L. Deng, K. G. Prashanth, S. Pauly, J. Eckert, and S. Scudino. 2018. "Microstructure and Mechanical Properties of Al-Cu Alloys Fabricated by Selective Laser Melting of Powder Mixtures." *Journal of Alloys and Compounds* 735: 2263–66. https://doi.org/10.1016/j.jallcom.2017.10.168.

Bartkowiak, Konrad, Sven Ullrich, Thomas Frick, and Michael Schmidt. 2011. "New Developments of Laser Processing Aluminium Alloys via Additive Manufacturing Technique." *Physics Procedia* 12 (PART 1): 393–401. https://doi.org/10.1016/j.phpro.2011.03.050.

Brandl, Erhard, Ulrike Heckenberger, Vitus Holzinger, and Damien Buchbinder. 2012. "Additive Manufactured AlSi10Mg Samples Using Selective Laser Melting (SLM): Microstructure, High Cycle Fatigue, and Fracture Behavior." *Materials and Design* 34: 159–69. https://doi.org/10.1016/j.matdes.2011.07.067.

Buchbinder, D., H. Schleifenbaum, S. Heidrich, W. Meiners, and J. Bültmann. 2011. "High Power Selective Laser Melting (HP SLM) of Aluminum Parts." *Physics Procedia* 12 (PART 1): 271–78. https://doi.org/10.1016/j.phpro.2011.03.035.

K. Kempen, L. Thijs , E. Yasa, M. Badrossamay, W. Verheecke and J.-P. Kruth, Department. 2011. "Process Optimization and Microstructural Analysis for Selective Laser." 484–95.

Lewandowski, John J., and Mohsen Seifi. 2016. "Metal Additive Manufacturing: A Review of Mechanical Properties." *Annual Review of Materials Research* 46 (1): 151–86. https://doi.org/10.1146/annurev-matsci-070115-032024.

Deng, Y., Yang, Y., Gao, C., Feng, P., Guo, W., He, C., Chen, J. and Shuai, C., 2018. "Mechanism for corrosion protection of β-TCP reinforced ZK60 via laser rapid solidification." International Journal of Bioprinting, 4(1):124.

Sing, S.L., Wang, S., Agarwala, S., Wiria, F.E., Ha, T.M.H. and Yeong, W.Y., 2017. "Fabrication of titanium based biphasic scaffold using selective laser melting and collagen immersion." International Journal of Bioprinting, vol.3 (1): 65–71.

Mondolfo, L. F. 1976. *Aluminium Alloys : Structure and Properties.* Edited by APA. 16th ed. London: Butterworth.

Polmear, I. J. 1995. *Light Alloys : Metallurgy of the Light Metals*. 3rd ed. London: Butterworth.